http://dx.doi.org/10.5012/bkcs.2013.34.12.3654

Gadolinium Complex of 1,4,7,10-Tetraazacyclododecane-1,4,7-trisacetic acid (DO3A) Conjugate of [(*p*-aniline benzothiazole)methyl]pyridine as a Tumor-Targeting MRI Contrast Agent

Ki Soo Nam, Ki-Hye Jung, Yongmin Chang,[†,‡,*] and Tae-Jeong Kim[*]

Department of Applied Chemistry, Kyungpook National University, Daegu 702-701, Korea
[*]E-mail: tjkim@knu.ac.kr
[†]Department of Medical & Biological Engineering, Kyungpook National University, Daegu 702-701, Korea
[‡]Department of Diagnostic Radiology & Molecular Medicine, Kyungpook National University, Daegu 702-701, Korea
[*]E-mail: ychang@knu.ac.kr
Received August 22, 2013, Accepted September 13, 2013

The synthesis of a DO3A conjugate of [(*p*-aniline benzothiazole)methyl]pyridine ($\mathbf{L^2}H_3$) and its gadolinium complex of the type [Gd($\mathbf{L^2}$)(H_2O)] (Gd$\mathbf{L^2}$) is described. The R_1 relaxivity (= 4.50 $mM^{-1}sec^{-1}$) and kinetic inertness of Gd$\mathbf{L^2}$ compares well with those of structurally analogous Dotarem® (R_1 = 3.70 $mM^{-1}sec^{-1}$), a typical extracellular (ECF) MRI contrast agent (CA). Yet, by comparison with Dotarem®, Gd$\mathbf{L^2}$ exhibits non-covalent interactions with human serum albumin (HSA) as evidenced by the ε* titration curve along with *in vivo* MR signal enhancement in both aorta and heart. Liver-specific nature of Gd$\mathbf{L^2}$ is also observed as excretion is made through gallbladder. Most notably, Gd$\mathbf{L^2}$ further demonstrates specificity toward the MDA-MB-231 breast cancer.

Key Words : Gadolinium, DO3A, Aniline benzothiazole, MRI, Tumor-targeting

Introduction

Magnetic resonance imaging (MRI) is a powerful technique for noninvasive diagnosis of the human anatomy, physiology, and pathophysiology on the basis of superior spatial resolution and contrast useful in providing anatomical and functional images of the human body.[1] At the clinical level, MRI techniques are mostly performed employing Gd-chelates to enhance the image contrast by increasing the water proton relaxation rate in the body.[2] Despite their wide and successful applications in clinics, however, conventional Gd-based low-molecular weight contrast agents are mostly ECF agents exhibiting rapid extravasation from the vascular space. As a result, the time window for imaging is considerably reduced, thus limiting acquisition of high-resolution images.

To overcome such limitations inherent to ECF MRI CAs, there has risen the necessity for the development of new MRI CAs carrying some unique functionalities. As a representative example, one may cite the so-called 'targeting MRI CAs' capable of responding to particular pathologies (*i.e.*, tumors, angiogenesis, apoptosis).[3-6] It would be even more desirable to equip the targeting imaging probes with such an additional function as therapy within a single molecule, from which a new term 'theranostic' (a coinage of diagnostic and therapeutic) may be derived.

We have recently reported the synthesis of DO3A-(*p*-aniline benzothiazole) conjugate ($\mathbf{L^1}H_3$) (Chart 1) and its Gd complex of the type [Gd($\mathbf{L^1}$)(H_2O)] (Gd$\mathbf{L^1}$) and demonstrated that Gd$\mathbf{L^1}$ is truly a single molecule theranostic agent.[7] Gd$\mathbf{L^1}$ is not only tumor-specific but also intracellular, enhancing MR images of cytosols and nuclei of tumor cells such as MCF-7, MDA-MB-231, and SK-HEP-1. Both $\mathbf{L^1}H_3$ and Gd$\mathbf{L^1}$ reveal antiproliferative activities as demonstrated by GI_{50} and TGI values obtainable from the cell counting kit-8 (CCK-8) assays performed on these cell lines. *Ex vivo* and *in vivo* monitoring of tumor sizes provide parallel and supportive observations for such antiproliferative activities.

Benzothiazole derivatives exhibit diverse biological properties such as anti-inflammatory, antimicrobial, and anti-cancer effects. As such, a great deal of research activities has been carried out in the past two decades in an effort to develop various benzothiazole derivatives with high anti-tumor activity.[8] Their antitumor properties have been utilized in combination with molecular imaging and therapy. For

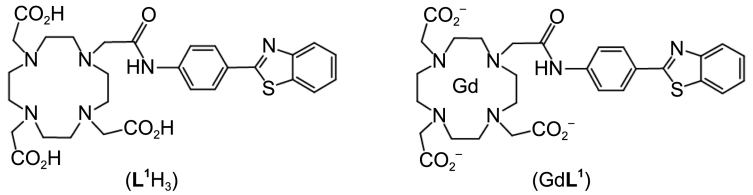

Chart 1

instance, radioactive Gp 7 complexes (M = ^{99m}Tc, ^{186}Re, ^{188}Re) have been proposed as potential radiopharmaceuticals for single photon emission computed tomography (SPECT) and radioimmunotherapy (RIT).[9,10] Benzothaizoles labeled with radioisotopes such as ^{99m}Tc and ^{11}C have been proposed as potential probes for Ab-amyloid plaques in the brain.[11,12] More recently, DO3A conjugates of benzothiazoles have been employed as multimodal imaging probes such as magnetic resonance imaging (MRI)/optical and MRI/SPECT.[13,14]

Motivated by such intriguing properties of benzothiazoles and by our recent observations cited above in connection with Gd**L**^{1}, we have decided to pursue further studies on the structure activity relationship for the theranostic application of benzothiazole derivatives. Here we wish to report the synthesis and evaluation of **L**^{2}H$_3$ and Gd**L**^{2} as a potential theranostic agent.

Experimental

General. All reactions were performed under an atmosphere of dinitrogen using the standard Schlenk technique. Solvents were purified and dried using standard procedures. DO3A(^{t}Bu)$_3$ (= 1,4,7,10-tetraazacyclododecane-1,4,7-tris-*tert*-butyl acetate) was prepared according to the literature method.[15] All other reagents were purchased from commercial sources and used as received unless otherwise stated. Deionized water was used throughout all experiments. The ^{1}H NMR experiments were performed on a Bruker Advance 400 Spectrometer by Center for Instrumental Analysis, Kyungpook National University (KNU). Chemical shifts were given as δ values with reference to tetramethylsilane (TMS) as an internal standard. Coupling constants are in Hz. FAB-mass spectra were obtained by using a JMS-700 model (Jeol, Japan) mass spectrophotometer by Korea Basic Science Institute (KBSI). Elemental analyses were conducted by using a Fisons EA 1108 model at Center for Instrumental Analysis, KNU.

Synthesis of 1,4,7,10-Tetraazacyclododecane-1,4,7-tris-*tert*-butyl acetate-10-[(6-bromomethylpyridyl)-2-methyl] (1). To a solution of 2,6-bis(bromomethyl)pyridine (1.0 g, 3.9 mmol) and K_2CO_3 (1.2 g, 8.6 mmol) in CH_3CN (50 mL) was added drop wise a solution of DO3A(^{t}Bu)$_3$ (1.1 g, 7.8 mmol) in CH_3CN (50 mL) at 0 °C. After the addition was complete, the reaction mixture was stirred for 18 h at 45 °C, after which solids were removed by filtration. The filtrate was evaporated under a reduced pressure. The crude compound was purified by chromatography (CH_2Cl_2/MeOH, 97:3) to give an ivory solid. Yield: 0.86 g (64%). ^{1}H NMR ($CDCl_3$) δ 7.76-7.73 (*t*, 1H, pyridine), 7.41-7.39 (*d*, 1H, pyridine), 7.26-7.24 (*d*, 1H, pyridine), 4.51 (s, 2H, C*H*$_2$Br), 3.58-2.13 (*m*, 22H, C*H*$_2$ in the cyclen ring), 1.51 (*s*, 9H, C*H*$_3$), 1.42 (*s*, 18H, C*H*$_3$). Anal. Calcd for $C_{33}H_{56}BrN_5O_6$·1.5HBr: C, 48.33; H, 7.07; N, 8.54. Found: C, 48.74; H, 7.05; N, 8.71. MALDI-TOF MS (*m*/*z*): calcd for $C_{33}H_{56}BrN_5O_6$: 698.7316 ([MH$^+$]). Found: 698.8658 ([MH$^+$]).

Synthesis of 10-{[6-(*p*-Aniline benzothiazole)methyl-pyridyl]methyl}-1,4,7,10-tetraazacyclododecane-1,4,7-tris-*tert*-butyl acetate (2). To a mixture of **1** (1.0 g, 3.9 mmol) and K_2CO_3 (1.0 g, 1.9 mmol) in acetone (50 mL) was added drop wise a solution of 2-(*p*-aniline)benzothiazole (0.8 g, 3.4 mmol) in acetone (100 mL). On completion of addition, the reaction mixture was stirred for 18 h at 45 °C, after which any solids were removed by filtration. The filtrate was evaporated under a reduced pressure. The crude compound was purified by chromatography (CH_2Cl_2/MeOH, 98:2) to give a paled yellow solid. Yield: 1.4 g (58%). ^{1}H NMR ($CDCl_3$) δ 7.98-7.96 (*d*, 1H, benzothiazole), 7.84-7.79 (*t*, 1H, pyridine), 7.68-7.61 (*d*, 1H, benzothiazole), 7.46-7.40 (*d*, 1H, pyridine), 7.38-7.28 (*m*, 2H, benzothiazole), 7.18-7.15 (*d*, 1H, pyridine), 6.74-6.66 (*d*, 2H, benzothiazole), 4.52-4.50 (*d*, 2H, benzothiazole), 3.19-1.78 (*m*, 24H, C*H*$_2$ in the cyclen ring), 1.49 (*m*, 27H, C*H*$_3$ in the cyclne ring). Anal. Calcd for $C_{46}H_{65}N_7O_6S$·2HBr: C, 54.92; H, 6.71; N, 9.75; S, 3.19. Found: C, 54.71; H, 6.60; N, 9.78; S, 2.50.

Synthesis of L^{2}H$_3$. Deprotection of the *tert*-butyl groups from **2** was performed as follows: The compound **2** (0.8 g, 1.9 mmol) was added to a solution of TFA/CH_2Cl_2 (1:3, 20 mL), and the mixture stirred at RT for 24 h. The solvents were removed by evaporation, the crude product dissolved in MeOH (5 mL), and diethyl ether (100 mL) added to precipitate an off-white solid. Yield: 0.6 g (96%). ^{1}H NMR (Methanol-d_4) δ 7.98-7.96 (*d*, 1H, benzothiazole), 7.84-7.77(*t*, 1H, pyridine), 7.65-7.62 (*d*, 1H, benzothiazole), 7.46-7.41 (*d*, 1H, pyridine), 7.38-7.28 (*m*, 2H, benzothiazole), 7.18-7.15 (*d*, 1H, pyridine), 6.74-6.66 (*d*, 2H, benzothiazole), 4.55-4.52 (*d*, 2H, benzothiazole), 3.19-1.78 (*m*, 24H, C*H*$_2$ in the cyclen ring). Anal.Calcd for $C_{34}H_{41}N_7O_6S$·5H_2O: C, 55.95; H, 6.49; N, 13.43; S, 4.39. Found: C, 56.40; H, 6.01; N, 13.66; S, 4.30. HR-FABMS (*m*/*z*): calcd for $C_{34}H_{41}N_7O_6S$: 676.2917 ([MH]$^+$). Found: 676.2914 ([MH]$^+$).

Synthesis of GdL^{2}. To a solution of **L**^{2}**H$_3$** (0.75 g, 0.74 mmol) in water (20 mL), was added $GdCl_3$·6H_2O (0.41 g, 0.74 mmol). The mixture was stirred at RT for 18 h during which time pH of the solution was periodically adjusted to 7.0-7.5 with NaOH (1.0 M). Water was removed by evaporation, the remaining oily residue taken up in a minimum amount of MeOH (~5 mL), and ether added drop wise for precipitation. The pale yellow solid thus formed was removed by filtration, washed with diethyl ether, and dried under vacuum. The absence of the free Gd^{3+} ion in the precipitate was confirmed by the xylenol orange test. The final product was obtained as a hygroscopic off-white solid. Yield: 0.4 g (67%). Anal. Calcd for $Gd_{34}H_{40}N_7O_7S$·9H_2O: C, 40.42; H, 5.72; N, 9.71; S, 3.17. Found: C, 39.96; H, 4.37; N, 9.61; S, 2.87. HR-FABMS (*m*/*z*): calcd for $Gd_{34}H_{40}N_7O_7S$: 830.1845 ([MH]$^+$). Found: 831.1926 ([MH]$^+$).

Transmetallation Kinetics and Determination of Kinetic Constants. These experiments were performed following the procedure described in the literature.[16,17] It is based on the evolution of the water proton relaxation rate (R_1^P) of a buffered solution (phosphate buffer, pH 7.4) containing Gd complex (2.5 mM) and $ZnCl_2$ (2.5 mM). The solution was made by adding a solution of 250 mmol/L solution of $ZnCl_2$ (10 μL, 250 mM) to a buffered solution of the Gd complex

(1.0 mL). After stirring the mixture vigorously, an aliquot of 300 μL was taken up for the relaxometric study. A control study, run on Gadovist®, Primovist®, Multihance®, Omniscan®, and Dotarem® with zinc acetate, has given results identical to those obtained in the presence of $ZnCl_2$. The R_1^P relaxation rate was obtained after subtraction of the diamagnetic contribution of the proton water relaxation from the observed relaxation rate $R_1 = (1/T_1)$. The measurements were performed on a 3 T whole body system (Magnetom Tim Trio, siemens, Germany) at room temperature.

Relaxivity. T_1 measurements were carried out using an inversion recovery method with a variable inversion time (TI) at 1.5 T (64 MHz). The magnetic resonance (MR) images were acquired at 35 different TI values ranging from 50 to 1750 msec. T_1 relaxation times were obtained from the non-linear least square fit of the signal intensity measured at each TI value. For T_2 measurements the CPMG (Carr-Purcell-Meiboon-Gill) pulse sequence was adapted for multiple spin-echo measurements. Thirty four images were acquired with 34 different echo time (TE) values ranging from 10 to 1900 msec. T_2 relaxation times were obtained from the non-linear least squares fit of the mean pixel values for the multiple spin-echo measurements at each echo time. Relaxivities (R_1 and R_2) were then calculated as an inverse of relaxation time per mM. The determined relaxation times (T_1 and T_2) and relaxivities (R_1 and R_2) are finally image-processed to give the relaxation time map and relaxivity map respectively.

***In vivo* MR Imaging and Image Analysis.** All animal experiments were performed in accordance with the rules of the animal research committee of Kyungpook National University. Six-week male. (Iinstiture of Cancer Resarch) ICR mice with weights of 29-31 g were for the MRI. The mice were anesthetized by 1.5% isoflurane in oxygen. Measurements were made before and after injection of Gd**L**^{2}, Primovist® and Multihance® *via* tail vein. The amount of CA per each injection was 0.1 mmol [Gd]/kg for MR images. After each measurement, the mouse was revived from anesthesia, and placed in the cage with free access to food and water. During these measurements, the animals were maintained at approximately 37 °C using a warm water blanket. MR images were taken with an 1.5 Tesla (T) MR unit (GE Healthcare, Milwaukee, WI, USA) equipped with a home-made small animal RF coil. The coil was of the receiver type with its inner diameter being 50 mm. The imaging parameters for SE (Spin Echo) are as follows: repetition time (TR) = 300 ms; echo time (TE) = 13 ms; 7 mm field of view (FOV); 192 × 128 matrix size; 1.2 mm slice thickness; number of acquisition (NEX) = 8. Images were obtained for 300 min after injection. The anatomical locations with enhanced contrast were identified with respect to heart, kidney and liver on post-contrast MR images. For quantitative measurement, signal intensities in specific regions of interest (ROI) measured using Advantage Window software (GE Medical, USA). The CNR (Contrast to Noise Ratio) was calculated using Eq. (1), where SNR is the signal to noise ratio.

$$CNR = (SNR_{post} - SNR_{pre}) \quad (1)$$

Results and Discussion

Synthesis. Scheme 1 shows the preparative method leading to the formation of a new bifunctional chelate (BFC) **L**^{2}H$_3$ and its gadolinium complex Gd**L**^{2}. A simple reflux of an equimolar mixture of 2,6-bis(bromomethyl)pyridine and DO3A(^{t}Bu)$_3$ in CH_3CN resulted in the monoalkylation to yield 6-bromomethylpyridyl-2-methyl-DO3A(^{t}Bu)$_3$ which was further treated with 2-(4-aminophenyl)benzothiazole (BTA) to give the DO3A(^{t}Bu)$_3$ conjugate of pyridylmethyl-BTA. Subsequent deprotection by TFA led to the formation of **L**^{2}H$_3$. The corresponding Gd complex (Gd**L**^{2}) is obtained

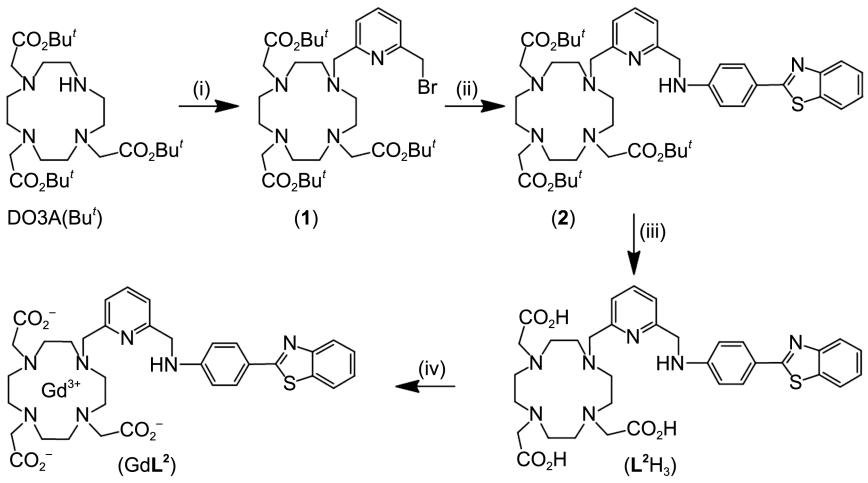

Conditions: (i) 2,6-bis(bromomethyl)pyridine, K_2CO_3, CH_3CN, 50 °C, 18 h;
(ii) 2-(4-aminophenyl)benzothiazole, acetone, K_2CO_3, 40 °C, 18 h;
(iii) TFA, CH_2Cl_2, RT, 24 h; (iv) $GdCl_3$, pH 7.0, RT, 18 h.

Scheme 1

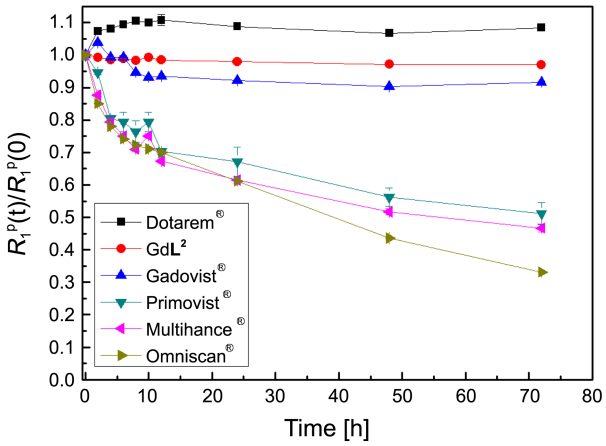

Figure 1. Evolution of longitudinal relaxation rates $R_1^P(t)/R_1^P(0)$ as a function of time for various MRI CAs ($[Gd]_0$ and $[ZnCl_2]_0$ = 2.5 mM in PBS (pH 7.4) at 128 MHz and 293 K).

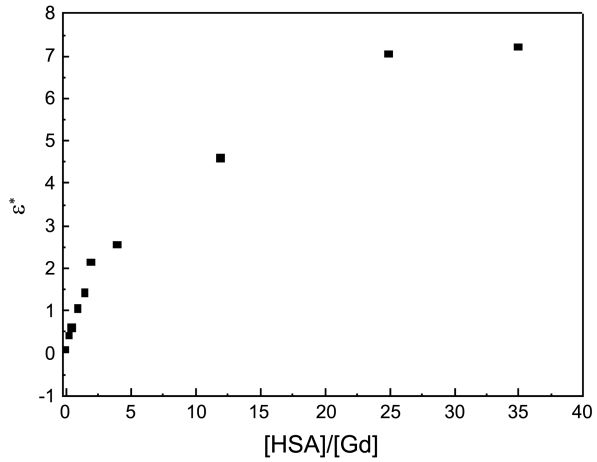

Figure 2. The plot of ε* values against [HSA]/[Gd] at 37 °C in phosphate-buffered saline (pH 7.4) for a 0.1 mmolar solution of Gd(DO3A-Py-BTA) and 0-22.5% w/v HSA at 64 MHz.

by simple complexation with an equimolar amount of gadolinium chloride in water. The complex was isolated as an off-white, hygroscopic solid by repeated precipitation with diethyl ether from the reaction mixture. All new compounds were characterized by microanalysis and various spectroscopic techniques such as ^{1}H NMR and HR-FAB mass spectroscopy.

Kinetic Inertness. The kinetic inertness of Gd**L**^{2} is represented by the evolution of the normalized paramagnetic longitudinal relaxation rates, $R_1^P(t)/R_1^P(0)$ as a function of time (Figure 1). Here, the relative value of R_1^P at any time t is a good estimator of the extent of transmetallation of gadolinium by zinc: GdL + Zn^{2+} → Gd^{3+} + $[ZnL]^{-1}$. Of various endogenous ions, Zn(II) has been noted to displace more gadolinium ions due to its higher concentration in the blood than any other ions such as Cu(II), Ca(II), K(I).[16] Quite expectedly, Gd**L**^{2} exhibits high kinetic stability comparable with those of Gadovist® and Dotarem® employing the same type of macrocyclic chelate DO3A and DOTA (= 1,4,7,10-tetraazacyclododecane-1,4,7,10-tetrakisacetic acid), respectively. Virtually no significant change in R_1 relaxivity is observed either with DO3A or DOTA for as long as 3 days. In contrast, however, other MRI CAs such as Multihance®, Primovist®, and Omniscan®, all employing the acyclic DTPA (= diethylenetriaminepentaacetic acid) analogues show significant drops in R_1 for the same period of time. Thus, it can be seen that the macrocyclic effect is obviously operative in the case of kinetic stability as well as thermodynamic one.

Relaxivity. The R_1 relaxivity in water of Gd**L**^{2} compares well enough with Dotarem®, Multihance®, and Primovist® (Table 1). In general, relaxivities drop when measured in PBS (pH 7.4) due to the formation of solid gadolinium phosphate which precipitates out of the solution. For the reason unknown to us, such a drop was more dramatic with Gd**L**^{2} (to exhibit R_1 as low as 1.0 $mM^{-1}s^{-1}$) than with Dotarem®, Multihance®, and Primovist®.

Table 1. Relaxivity data of Gd**L**^{2}, Dotarem®, Primovist®, and Multihance® in water (64 MHz, 293 K)[a]

	R_1 ($mM^{-1}s^{-1}$)	R_2 ($mM^{-1}s^{-1}$)
1	4.5 (1.2)	3.5 (1.9)
Dotarem®	3.7 (3.7)	4.1 (4.0)
Primovist®	7.1 (6.6)	8.0 (7.0)
Multihance®	5.4 (5.1)	7.0 (5.4)

[a]Vaues in parentheses are those measured in PBS.

Interaction with HSA. The evidence for the non-covalent lipophilic interactions between Gd**L**^{2} and HSA can be adequately provided by the so-called ε* titration (Figure 2). The curve represents the extent of relaxation enhancement as a function of the HSA concentration. A non-linear increase in the ε* value with an increase in the HSA concentration typically indicates the presence of protein binding.[18]

***In vivo* MRI.** *In vivo* coronal images of mice obtained by tail vein injection with Gd**L**^{2} reveal strong signal enhancement in liver, heart, and abdominal aorta (Figure 3). Gallbladder is also enhanced 40 minutes after injection

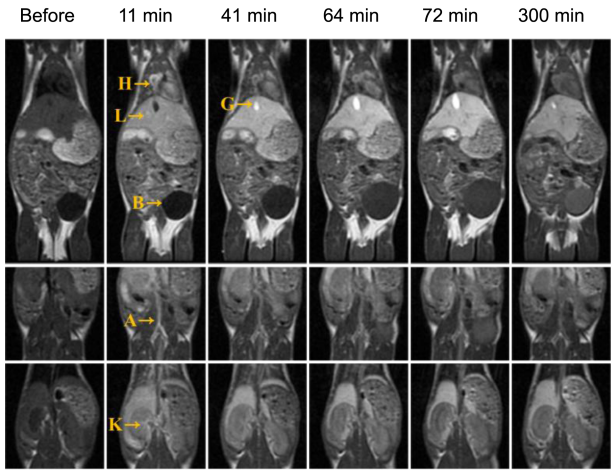

Figure 3. *In vivo* MR T_1 weighted spin echo (SE) coronal images of mice obtained by tail vein injected with Gd**L**^{2} (0.1 mmol/kg): H, heart; L, liver; B, bladder, G, gallbladder; A, abdominal aorta; K, kidney (64 MHz).

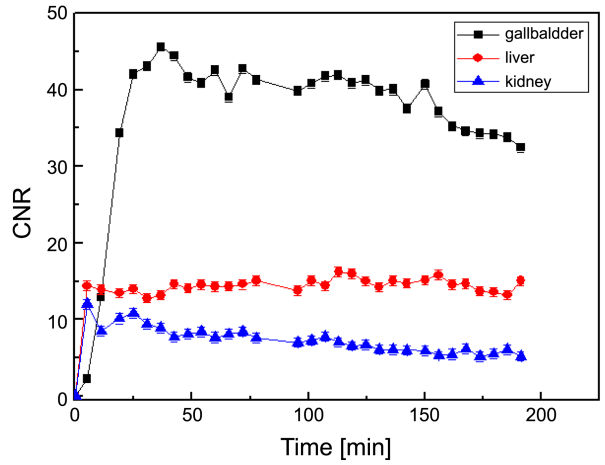

Figure 4. CNR profiles obtained by Gd**L**^{2} for liver, gallbladder, and kidney.

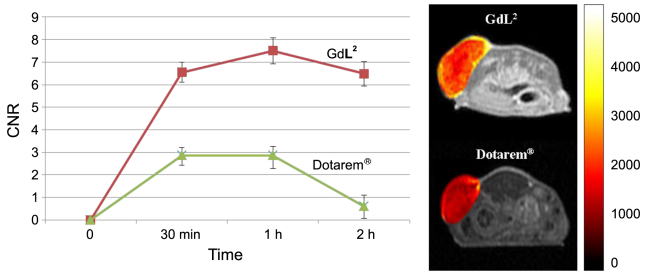

Figure 5. CNR profiles and *in vivo* MR axial images of mice bearing MDA-MB-231 tumor obtained with Gd**L**^{2} and Dotarem® (0.1 mmol [Gd]/kg).

indicating excretion is partially made through bile *via* hepatocyte in addition to the ordinary renal excretion. The contrast-to-noise ratio (CNR) curve provides a supporting evidence for the bile excretion (Figure 4).

Tumor Targeting. Gd**L**^{2} shows a strong affinity toward the MDA-MB-231 tumor cell as observed from the *in vivo* CNR profiles along with MR images (Figure 5). The maximum intensity endures for as long as 2 h in contrast to Dotarem®, most of which excretes out of the body within 2 h.

Judging from our previous observations that Gd**L**^{1} possesses antiproliferative properties against a series of tumors, structurally related Gd**L**^{2} is considered to reveal similar behaviors as a single molecule theranostic agent. In this regard, it is to be highly recommended to pursue further a study on the structure-activity relationship (SAR) with Gd**L**^{2}, which is the subject of our future communication.

Conclusions

In conclusion, we have prepared DO3A conjugate of pyridylbenzothaizole (**L**^{2}H$_3$) and its gadolinium complex of the type [Gd(**L**^{2})(H$_2$O)] (Gd**L**^{2}). The R_1 relaxivity and kinetic stability of Gd**L**^{2} compare well with clinically available ECF MRI CAs such as Dotarem® and Gadovist®. *In vivo* MR images of mice with Gd**L**^{2} show strong signal enhancement in gallbladder and aorta as well as liver, heart, and kidney. Further, Gd**L**^{2} shows a strong affinity toward the MDA-MB-231 tumor cell.

Acknowledgments. T.-J.K. gratefully acknowledges the NRF for financial support (Grant No. 2012-0006388). NMR and mass spectral measurements were performed by KBSI. We thank Dr. Ji-Ae Park (Molecular Imaging Research Center, Korea Institute of Radiological and Medical Sciences) for some valuable experiments.

References

1. Caravan, P. *Chem. Soc. Rev.* **2006**, *35*, 512.
2. Caravan, P.; Ellison, J. J.; McMurry, T. J.; Lauffer, R. B. *Chem. Rev.* **1999**, *99*, 2293.
3. Aime, S.; Botta, M.; Garino, E.; Crich, S. G.; Giovenzana, G.; Pagliarin, R.; Palmisano, G.; Sisti, M. *Chem.-Eur. J.* **2000**, *6*, 2609.
4. Chong, H. S.; Song, H. A.; Ma, X.; Lim, S.; Sun, X.; Mhaske, S. B. *Chem. Commun.* **2009**, 3011.
5. Barrio, J. R.; Satyamurthy, N.; Huang, S.-C.; Petri, A.; Small, G. W.; Kepe, V. *Acc. Chem. Res.* **2009**, *42*, 842.
6. Tweedle, M. F. *Acc. Chem. Res.* **2009**, *42*, 958.
7. Kim, T.-J. Manuscript submitted to *J. Med. Chem.*.
8. Bradshaw, T. D.; Westwell, A. D. *Curr. Med. Chem.* **2004**, *11*, 1241.
9. Tzanopoulou, S.; Pirmettis, I. C.; Patsis, G.; Paravatou-Petsotas M. P.; Livaniou, E.; Papadopoulos, M.; Pelecanou, M. *J. Med. Chem.* **2006**, *45*, 5408.
10. Tzanopoulou, S.; Sagnou, M.; Paravatou-Petsotas, M.; Gourni, E.; Loudos, G.; Xanthopoulos, S.; Lafkas, D.; Kiaris, H.; Varvarigou, A.; Pirmettis, I. C.; Papadopoulos, M.; Pelecanou, M. *J. Med. Chem.* **2010**, *53*, 4633.
11. Chen, X.; Yu, P.; Zhang, L.; Liu, B. *Bioorg. Med. Chem. Lett.* **2008**, *18*, 1442.
12. Mathis, C. A.; Wang, Y.; Holt, D. P.; Huang, G.-F.; Debnath, M. L.; Klunk, W. E. *J. Med. Chem.* **2003**, *46*, 2740.
13. Martins, A. F.; Morfin, J.-F.; Kubíčková, A.; Kubíček, V.; Buron, F.; Suzenet, F.; Salerno, M.; Lazar, A. N.; Duyckaerts, C.; Arlicot, N.; Guilloteau, D.; Geraldes, C. F. G. C.; Tóth, É. *ACS Med. Chem. Lett.* **2013**, *4*, 436.
14. Saini, N.; Varshney, R.; Tiwari, A. K.; Kaul, A.; Allard, M.; Ishar, M. P.; Mishra, A. K. *Dalton Trans.* **2013**, *42*, 4994.
15. Gu, S.; Kim, H. K.; Lee, G. H.; Kang, B. S.; Chang, Y.; Kim, T. J. *J. Med. Chem.* **2011**, *54*, 143.
16. Laurent, S.; Elst, L. V.; Copoix, F.; Muller, R. N. *Invest. Radiol.* **2001**, *36*, 115.
17. Tweedle, M. F.; Hagan, J. J.; Kumar, K.; Mantha, S.; Chang, C. A. *Magn. Res. Imaging* **1991**, *9*, 409.
18. Caravan, P.; Cloutier, N. J.; Greenfield, M. T.; McDermid, S. A.; Dunham, S. U.; Bulte, J. W. M.; Amedio, J. C.; Looby, R. J.; Supkowski, R. M.; Horrocks, W. D., Jr.; McMurry, T. J.; Lauffer, R. B. *J. Am. Chem. Soc.* **2002**, *124*, 3152.